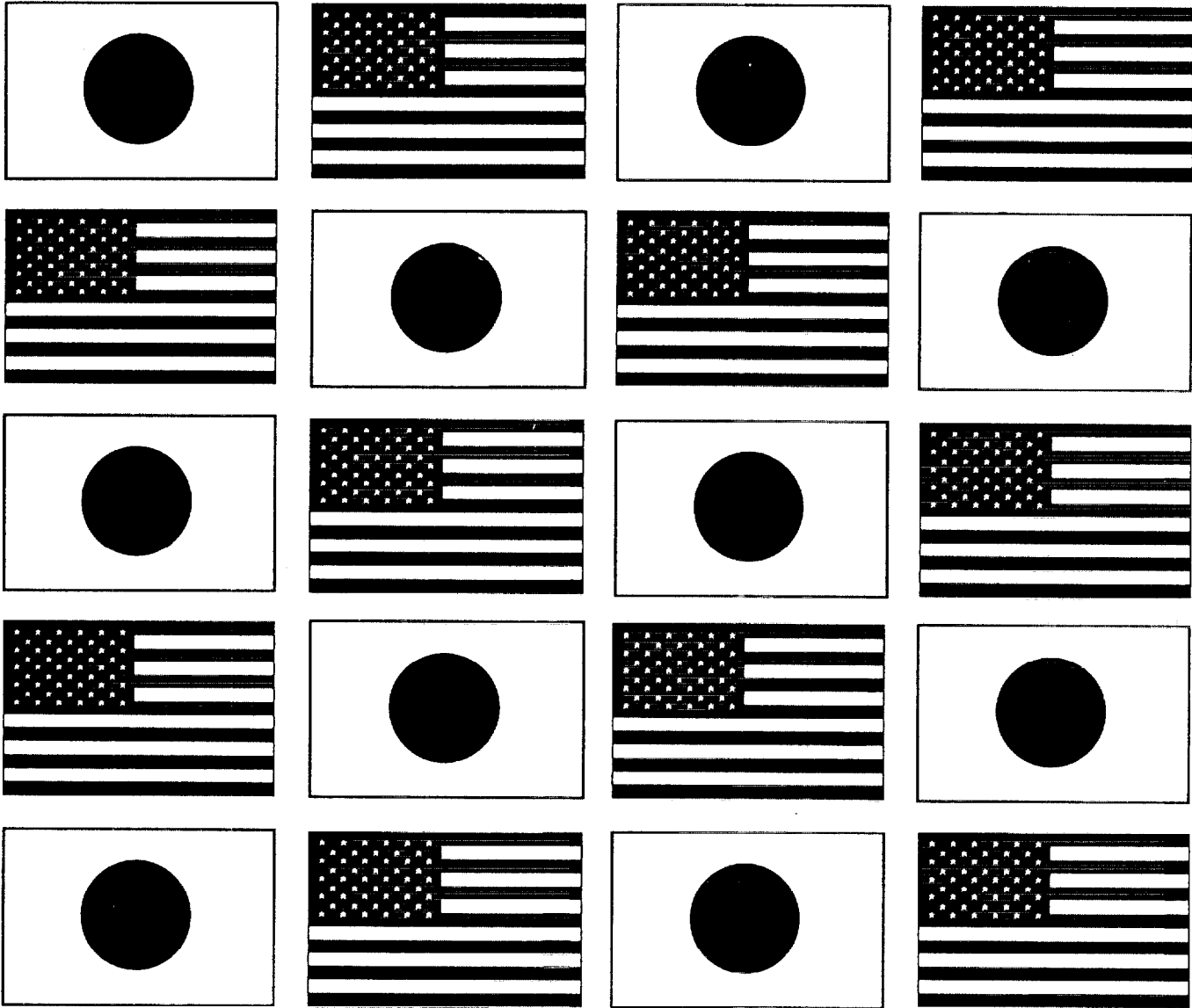


# Wind and Seismic Effects

Proceedings of the 30th Joint Meeting

NIST SP 931



U.S. DEPARTMENT OF COMMERCE  
Technology Administration  
National Institute of Standards and Technology

# Wind and Seismic Effects

**NIST SP 931**

---

**PROCEEDINGS OF  
THE 30TH JOINT  
MEETING OF  
THE U.S.-JAPAN  
COOPERATIVE PROGRAM  
IN NATURAL RESOURCES  
PANEL ON WIND AND  
SEISMIC EFFECTS**

**Issued August 1998**

**Noel J. Raufaste  
EDITOR**

**Building and Fire Research Laboratory  
National Institute of Standards and Technology  
Gaithersburg, MD 20899**



**U.S. DEPARTMENT OF COMMERCE  
William M. Daley, Secretary**

**TECHNOLOGY ADMINISTRATION  
Gary R. Bachula, Acting Under Secretary for Technology**

**National Institute of Standards and Technology  
Raymond G. Kammer, Director**

---

# **EARTHQUAKE ENGINEERING**

**Evaluation of the Seismic Capacity Of  
An Existing Thick Wall Reinforced Concrete Structure  
Using Probabilistic Criteria**

by

F. Loceff<sup>1</sup>, G. Mertz<sup>1</sup> and G. Rawls<sup>1</sup>

**ABSTRACT**

A seismic qualification of a reinforced concrete nuclear materials processing facility using performance based acceptance criteria is presented. Performance goals are defined in terms of a minimum annual seismic failure frequency. Pushover analyses are used to determine the building's ultimate capacity and relate the capacity to roof drift and joint rotation. Nonlinear dynamic analyses are used to quantify the building's drift versus earthquake magnitude using a suite of time histories representing varying soil conditions and levels of seismic hazard.

A probabilistic correlation between joint rotation and damage state is developed from experimental data. The results of the deterministic pushover and nonlinear time history analyses are evaluated statistically to develop a probability of seismic failure or fragility. The building fragility level is convolved with the seismic hazard curve to determine annual seismic failure frequency.

**KEYWORDS**

**BUILDING; FRAGILITY, NONLINEAR;  
SEISMIC**

**1. INTRODUCTION**

This paper discusses the seismic qualification of an existing nuclear material processing facility. This work was part of an effort to update the facility safety analysis

The material processing facility is a heavy concrete structure that was built in the early 1950's. Radiation shielding was the primary design consideration. Lateral load resistance was given scant attention in 1950's vintage design codes. This combination of factors resulted in large, lightly reinforced concrete sections which do not meet today's seismic detailing requirements.

The safety analysis is updated to include our current understanding of the seismic hazard at the building site and the building's seismic response. The current seismic design loading is several times larger than the lateral loads considered in the original design. When the current seismic loads are combined with the lack of current code detailing, the structure will not meet a design-code seismic qualification.

An probabilistic evaluation methodology that addresses the lightly reinforced concrete buildings with 1950's detailing, typically found in older facilities, is discussed in this paper. Using this methodology, the authors have shown that a nuclear material processing facility is capable of surviving the postulated design basis earthquake (DBE).

This paper emphasizes the probabilistic aspects of this evaluation while a companion paper (Mertz et al, 1998) emphasizes the analysis methodology.

---

<sup>1</sup> Westinghouse Savannah River Company, Aiken SC 29808.

## 1.1 ACCEPTANCE CRITERIA

DOE Standard 1020 sets acceptance criteria for DOE facilities based on performance goals. For the structure discussed in this paper the performance goal is an annual failure frequency of  $2 \times 10^{-4}$ . The standard allows considerable latitude in evaluation methodology as long as the specified performance goal for a given category of structures, systems and components (SSCs) are met. This latitude consists essentially of three approaches to meet the performance goals for the SSC.

- For a hazard probability specified for the facility use, apply conservative deterministic evaluation techniques based on national consensus standards as supplemented by DOE Standard 1020 requirements for the facility performance goal.
- Achieve less than a 10% probability of unacceptable performance of an SSC subjected to a scaled design basis earthquake (SDBE) that is 50% larger than the DBE.
- Demonstrate acceptable structural behavior by showing that the building annual probability of seismic failure is less than the facility performance goal.

A key factor in the probabilistic approach is the specification of an acceptance criteria, stated in probabilistic terms, that conforms to the performance goals in DOE Standard 1020.

The structure discussed in this paper consists of a reinforced concrete frame with partially developed joints. Failure for a specific joint is defined, in this paper, as the reduction of capacity below a nominal value. Frame failure is conservatively assumed to occur when the first joint fails. Thus, this probabilistic assessment has a definite conservative bias. Identifying a joint failure, as such, does not imply the failure of the building frame. In fact, substantial conservatism exists since a failure of the frame cannot occur until a sufficient number of joints sustain sufficient damage to cause a collapse mechanism.

Using this definition of unacceptable structural behavior, the evaluation methodology leads to the calculation of the conditional probability of seismic failure. This conditional failure probability is measured against the acceptance criteria in DOE Standard 1020.

## 1.2 ANALYSIS METHODOLOGY

There are several options available to evaluate older existing facilities for seismic loads. The choice should consider the in-situ building condition, the level of seismic load, the effects of foundation embedment, the functional requirements, the level of acceptable damage, the confinement requirements, and the performance category of the facility. This paper concentrates on the more rigorous approach to demonstrate the capability of a facility to withstand a postulated seismic event.

## 1.3 FACILITY DESCRIPTION

The material processing facility, designed and constructed in the early 1950s, are reinforced-concrete buildings. They are 66 ft high, 122 ft wide (Figure 1) and consist of eighteen segments, typically 43 ft long. One-inch expansion joints separate the segments from each other. The exterior walls range from 2.5 to 4.8 ft thick and support a haunched roof slab. A frame structure is contained within the building. The lower portion consists of continuous walls and discrete columns while the upper portions contain continuous walls. The specified design strength of the concrete is 2,500 psi and Grade-40 reinforcing steel was used. The structure is supported on a 5-foot-thick reinforced-concrete foundation mat. The total weight of a typical segment is 24,800 kips.

Primary longitudinal (N-S) stiffness against seismic loading comes from the 4 ft thick shear walls while the transverse (E-W) stiffness is provided by frame action of the reinforced-concrete walls.

The original design was based on the Uniform Building Code (UBC, 1946) with a 1951 Addenda and on the American Concrete Institute (ACI) Code ACI 318-47. The design focused on gravity loading with only a nominal seismic lateral load applied statically to the building structure. The exterior walls were

designed to resist a uniform external over-pressure. This design condition resulted in heavier reinforcement on the inside face of the walls than on the outside face. Many of the embedment and splice lengths of the reinforcing steel do not satisfy current ACI specifications with some embedment lengths only 25 percent of that required by the current code.

A typical joint that connects the roof to the exterior wall is shown in Figure 2. This joint was designed for gravity loads and the bottom slab reinforcing is not fully anchored in the wall. Seismic loads will cause load reversal, putting the bottom bars in tension and the capacity of this underdeveloped bar is reduced due to bond slip. This joint is 43 feet long and the geometry of the joint constrains the concrete around the reinforcing bar.

## 2. DEVELOPMENT OF SEISMIC INPUT

The probabilistic structural analysis requires that the median responses of the building be determined. The building sits on a deep layered site consisting of sands and clays over bedrock. Bedrock is approximately 950 ft below free field. Seismic motions were developed for: 1) an evaluation basis earthquake (EBE) with 2000 year return period, and 2) a seismic margin earthquake (SME) with a 10,000 year return period. Both the EBE and SME ground motions are defined in the form of 5% damped rock-outcrop response spectra. Eight acceleration time histories were prepared; four compatible with the EBE spectrum and four compatible with the SME spectrum.

To consider the variabilities in the soil between the free field and the bedrock each time history was convolved through several soil columns, as shown schematically in Figure 3. At the site, there were four deep borings ( $\cong 950$  ft) to bedrock, and five shallow borings, ( $\cong 150$  ft). Each EBE and SME time history was convolved through 20 soil columns that were formed by combining each deep boring with all five shallow borings, resulting in 80 time histories at the base of the building.

The response spectra of the convolved time histories are plotted at the elevation of the basemat of the building and a mean spectrum

was calculated for both the EBE and the SME motions. To reduce the computational effort in developing the building response, a subset of 11 out of 80 time histories were chosen for both the EBE and SME events. These 11 time histories were selected such that the mean of their response spectra closely matches the mean of the full suite of 80 time histories. Furthermore, the 11 spectra are evenly spaced between the maximum and minimum envelopes of the 80 spectra from the convolved time histories, and have an equal probability of occurrence.

The median response spectra of these time histories are shown in Figure 4 for the 2,000-year and the 10,000-year events.

## 3. DETERMINISTIC BUILDING RESPONSE

The building behavior was determined by performing a static pushover analysis to determine the structure's overall lateral load resistance. Nonlinear dynamic analyses, using a simplified dynamic model, were performed to determine the seismic response.

### 3.1 STATIC PUSHOVER ANALYSIS

In the east-west direction, the structure consists of a moment resisting lateral frame with a rigid penthouse structure. A static pushover analysis of the lateral load resisting frame is performed to determine the building's lateral load capacity and the relationship between displacement and joint rotation.

Lumped nonlinear springs are located at critical joints to represent, cracking of the gross section, yielding of the longitudinal reinforcing and bond slip due to inadequate development. In partially developed joints, the members' capacity is reduced by the ratio of the actual development length to the code development length.

A typical monotonic load-deformation curve or backbone curve for the structure is shown in Figure 5. The structure remains elastic below a base shear of about 5% of the building weight. Above this load, individual joints crack and yield at different load levels, which gradually soften the overall structural response. A plastic collapse mechanism is nearly formed after six

inches of displacement. For displacements beyond this point, the slight increase in capacity due to strain hardening of the reinforcement is nearly offset by the increasing P- $\Delta$  forces. The ultimate capacity corresponds to about 11% of the structure's weight.

### 3.2 NONLINEAR DYNAMIC ANALYSIS

A fragility analysis for a reinforced-concrete structure subjected to strong earthquake motions requires realistic conceptual structural models that consider changes in stiffness and material properties, the variability of seismic source and in-situ soil conditions. To adequately address these parameters, numerous non-linear time history analyses were performed. Since non-linear time history analyses are numerically intensive, reduced dynamic models are used to perform the analyses.

The elastic response of the frame in Figure 1 is dominated by the response of the first mode, with roof drifts in-phase with joint rotations. Thus, the structure is represented with a single-degree-of-freedom (SDOF) model having an equivalent elastic response as the full structural model. The elastic natural frequency of the structure is on the order of 1 to 1.3 Hz.

The nonlinear response of the SDOF model is represented by the Takeda hysteresis model (Takeda, 1970) that represents the experimentally observed behavior of reinforced concrete beams subject to cyclic loads. The 11 EBE and 11 SME ground motions are evaluated using a SDOF model which represent the nominal capacity of the building based on 'design' material properties. The range of roof displacements, for the 11 representative 2,000 and 11 representative 10,000 year ground motions is summarized in Table 1.

The initial structural stiffness of the SDOF model was also perturbed to address the uncertainty in natural frequency on response. The range of roof displacements for the 11 representative ground motions with lower bound (-30%), best estimate, and upper bound (+30%) stiffness is summarized in Table 2. This structure is more sensitive to variations in soil column than to variations of initial stiffness.

**Table 1 Range Of Roof Displacements For Different Earthquake Magnitudes and Soil Columns**

Ground Motion	#	Minimum (in)	Maximum (in)
EBE	33	1.30	2.78
SME	33	6.52	10.2

**Table 2 Range Of Roof Displacements For Different Earthquake Magnitudes, Soil Columns, And Natural Frequencies**

Ground Motion	#	Minimum (in)	Maximum (in)
EBE	33	1.30	2.78
SME	33	6.52	10.2

The 11 EBE ground motions were also evaluated using a SDOF model that represented the median building capacity to investigate the change in response with capacity. The lateral load capacity of the frame, calculated using median material properties, is about 27% larger than the lateral load capacity calculated using material properties that are exceeded by 95% of the test data. The influence of material strengths on the range of seismic displacement, shown in Table 3, is small because the structure is responding in the displacement controlled region of the spectra.

**Table 3 Range Of SME Roof Displacements For Different Material Strengths**

Material Properties	#	Minimum (in)	Maximum (in)
95% Exceedance	33	6.52	10.2
Median	33	7.21	10.1

Representative nonlinear MDOF were also performed to validate the SDOF analyses. These comparisons indicate that the SDOF mass

participation was overestimated and consequently, the SDOF models tend to over-predict the roof displacements.

#### 4. PROBABILISTIC ANALYSIS

Ground motions and the resulting structural drifts were developed in the proceeding sections. These values are combined in this section with the probability of joint failure to determine the mean annual probability of seismic failure which is compared to the structures performance goal specified by DOE Standard 1020.

##### 4.1 PROBABILITY OF PARTIALLY DEVELOPED JOINT FAILURE

Rotations are imposed on the joints when a frame drifts under seismic lateral loads. Joints that do not meet the ACI 318-95, development length requirements may not develop their full yield moment. In this evaluation, the ACI bond stress is used to limit the bending capacity ( $\phi M_n$ ), of a partially developed joint, by the ratio of actual development length, to the ACI development length. The amount of bar slip at the reduced moment is determined by the rotation imposed on the joint and ultimately by the lateral drift of the frame as shown in Figure 6. Failure is defined as the inability of a joint to resist the reduced moment, at a given drift.

Typical confined bar pullout test results (Eligehausen, 1983), are shown in Figure 7. Monotonic tests indicate that for low magnitudes of bond slip the bars have a much larger capacity than the ACI 318-95 code allows and that the code bond capacity corresponds to the capacity at large deformations. Cyclic tests indicate that the capacity degrades with an increasing number of cycles and the degradation is more pronounced when cycled with larger ranges of slip. After 10 cycles, the code capacity is obtained when loading beyond the maximum post-bond slip. This test data was reviewed and judged that 13% and 75% of the specimen would fail to maintain the ACI bond capacity at peak slip ranges of 0.2 in and 0.36 in respectively. A lognormal probability distribution is fit to these two failure estimates as shown in Figure 8.

Test of full scale joints with partially developed bars, shown in Figure 9 (Beres, 1992, Aycardi, 1992), demonstrate that the joint is capable of resisting considerable rotation at the reduced bending moment  $\phi M_n l/d$ . Joint rotations for this data are converted to bar slip, ranked, and used to validate the bar slip probability of failure in Figure 8. Note that the bar slip in Figure 6 is the product of joint rotation and the distance between the neutral axis to the reinforcing,  $d$ . A joint rotation of 0.02 radians of the 24 inch deep test specimen, in Figure 9, causes the same bond slip as a 0.01 radian rotation on a section that is 48 inches thick. Thus, allowable joint rotation limits should be viewed with caution when evaluating thick sections.

Individual joint rotations corresponding to each increment of roof drift in the pushover analysis, Figure 5, are converted into components of bending rotation and bond slip. Bond slip failure probabilities from Figure 8 are assigned to each joint based on the computed bar slip. Bending failure probabilities are also assigned using a similar relationship and combined with the bond slip failure probability. Bond slip dominated the failure probabilities of this structure.

It was assumed that the loss of any critical member in the load path could result in building failure, Therefore, an envelope of the individual critical member joint failure probabilities represents the probability of structural failure, and is shown in Figure 10. Parametric studies indicate that this indeterminate structure can survive the loss of a single critical joint with a reduced lateral load capacity. As shown above the seismic drift is insensitive to lateral load capacity because the building responds in the displacement controlled region of the spectra. Thus, the probability of structural failure, shown in Figure 10, has a conservative bias.

For roof displacements less than 4 inches (0.5% drift) the probability of failure is negligible while a roof displacement of 5.8 inches (0.8% drift) corresponds to a 50% probability of failure. The probability of failure for the structure is dominated by a joint on the exterior frame that fails by bond slip.

## 4.2 SEISMIC FRAGILITY

To evaluate the results of the structural analysis described above, to probabilistic acceptance criteria, an estimate of the conditional probability of seismic failure or fragility is calculated. The fragility analysis provides an estimate of the median seismic capacity (50 percent conditional probability of failure) and the associated uncertainty. The capacity for this analysis is defined in terms of the building drift. The drift is then correlated to a seismic ground motion parameter.

The fragility estimate for this evaluation is formulated as a log-normal distribution, which is mathematically expressed as:

$$P_f(\Delta) = \Phi \left[ \frac{\ln \frac{\Delta}{\Delta_m}}{\beta} \right] \quad (1)$$

where  $P_f(\Delta)$  = Conditional Probability of Failure

$\Delta_m$  = Median Drift

$\beta$  = Logarithmic Standard Deviation

$\Phi$  = Standard Normal (Gaussian) Distribution

A fragility curve for the structure is provided in Figure 11. The variability or uncertainty in the analysis is expressed through the logarithmic standard deviation or beta ( $\beta$ ) value. The variability is the slope of the fragility curve with larger  $\beta$  resulting in a flatter slope. In this analysis both the randomness in the earthquake motion and the lack of knowledge or uncertainty is treated as a combined variability.

The sources of variability in the analysis include the input time history motion, the structural stiffness, the strength of R/C sections, and the ground motion correlation equation. The variability for each of the above sources was combined using the square root of the sum of the squares method to obtain the combined variability.

The response variability due to input time history, structural stiffness and strength was calculated by performing a statistical analysis of the nonlinear SDOF drift data. In developing the drift data, 99 nonlinear time history calculations were performed. Three different combinations of concrete strength and earthquake annual probability were evaluated. These cases are identified in Table 4.

**Table 4 Nonlinear SDOF Analyses**

Case	Concrete Strength	EQ Return Period
1	95%	2,000 year
2	95%	10,000 year
3	50%	10,000 year

For each of the three cases and the 11 time histories described above, three different building stiffness (natural frequency) values were evaluated. The stiffness values correspond to the best estimate, the +30 percent and the -30 percent estimates. Therefore, for each case, 33 (11 time histories x 3 stiffness values) drift values were calculated. Each of the 33 drift values was considered to have an equal probability of occurrence.

The variation in the drift values,  $\beta_R$ , accounts for both the earthquake time history randomness and the structural stiffness uncertainty and was calculated by fitting the 33 data points from each of the three cases for nonlinear SDOF analysis to a log-normal distribution. The slope of the distribution provides the  $\beta$  value. The highest  $\beta_R$  value from the three cases is used in the fragility analysis. The larger  $\beta$  value will produce a flatter fragility curve that will result in a larger change in failure probability over a specified range of ground motion. In this analysis the  $\beta_R$  value was calculated to be 0.23.

The variability in strength ( $\beta_s$ ) is determined by performing two seismic analyses. The first analysis was performed using nominal material properties (95% exceedance) to calculate the ultimate strength, and the second analysis was based on median material properties. For a constant earthquake level, represented by Cases

2 and 3 in Table 4, the variability in a fragility analysis is measured by the change in building response due to the change in ultimate strength. The median drift values in cases 2 and 3 are the same because the building is responding in the displacement control region of the spectra. Thus, the variability for this structure with respect to strength is zero ( $\beta_s = 0$ ).

The fragility level for a structure is correlated to a ground motion parameter. Studies provided by Sozen, (Gulkan, 1974), Iwan, (Iwan, 1980), and Kennedy, (Kennedy, 1984), show that the drift of nonlinear SDOF systems can be reasonably correlated to the spectral displacement by the equation

$$\delta \approx S_D(f_e, \Delta_e) \quad (2)$$

Where  $S_D(f_e, \Delta_e)$  is the input ground motion spectral displacement at an effective frequency  $f_e$  and an effective damping  $\Delta_e$ .

The data in this analysis provided a good correlation between the average spectral displacement ( $\bar{S}_D$ ) taken over a frequency range from 0.35-0.65 Hz at an effective damping level of 10%. Therefore, the following equation was used to represent the drift response ( $\delta_R$ ) in terms of spectral displacement

$$\delta_R \approx \bar{S}_D \quad (3)$$

A small level of variability in the ground motion equation is addressed by assigning a beta value ( $\beta_{EQ}$ ) to the equation. Based on engineering judgement  $\beta_{EQ} = 0.05$  was assigned to the equation.

The median capacity of the structure is defined as the lateral drift that results in a 50% probability of structural failure. To develop the median capacity and the associated variability the drift verses probability of failure data in Figure 10 is fit to a log-normal distribution. The log-normal fit of the data provides a median drift capacity of 5.8 inches with an associated

variability on capacity  $\beta_C = 0.17$ . The median capacity of 5.8 inches represents a 50 percent probability of failure.

The variability for each individual source is summarized in Table 5. These variabilities were combined using square root of the sum of the squares as the statistical method to determine a composite variability. A composite variability of 0.29 is calculated for this structure.

**Table 5 Seismic Fragility**

Variability	Value
Response - $\beta_R$	0.23
Strength - $\beta_S$	0.00
Equation - $\beta_{EQ}$	0.05
Capacity - $\beta_C$	0.17
Composite - $\beta^*$	0.29

$$*\beta = \text{Composite Variability} = \sqrt{\beta_R^2 + \beta_S^2 + \beta_{EQ}^2 + \beta_C^2}$$

Comparing Figure 10 with Figure 11, the building median drift capacity of 5.8 inches and its associated variability  $\beta_C$  of 0.17, as shown in Figure 10, can be considered a lower bound fragility curve because it does not contain all of the sources of variability. The other sources of variability including response, strength, and ground motion correlation provide adjustments that flatten the distribution, as shown in Figure 11. The flattening of the fragility curve using the composite beta value of 0.29 results in a wider range on probability of failure verses seismic input motion. Correlating the drift response to the ground motion parameter spectral displacement completes the final seismic fragility for the structure. The seismic fragility for this structure is expressed in term of the spectral displacement by the equation:

$$S_D = \hat{S}_D e^{\beta x} \quad (4)$$

Where  $S_D$  = Spectral displacement at a given probability of failure

$\hat{S}_D$  = Median spectral displacement (5.8 inches)

$\beta$  = Composite variability (.29)

X = The number of normal standard deviations the given probability is from the median.

#### 4.3. ANNUAL PROBABILITY OF SEISMIC FAILURE

The fragility curves were convolved (integrated) with the site mean hazard curve to obtain an estimate of the mean annual probability of seismic failure. Equation 5, from DOE Standard 1020, is a good approximation for more formal numerical integration, was used.

$$P_r = \frac{H_D e^{\frac{1}{2}(K_H \beta)^2}}{\left(\frac{C_{50}}{SME}\right)^{K_H}} \quad (5)$$

Where  $P_r$  = Mean annual probability of seismic failure

$C_{50}$  = Median spectral displacement capacity

$\beta$  = Composite logarithmic standard deviation

SME = Median SME response

$H_D$  = Annual probability of exceeding the median SME

$K_H$  = Slope parameter of the spectral displacement hazard curve

This equation assumes that the fragility curve is log-normal and that the hazard curve of average spectral displacement can be approximated by a straight line on a log-log plot. Values summarized in Table 5 were used to calculate the mean annual probability of failure. For the structure evaluated in this analysis the mean annual probability of seismic failure was

determined to be  $1.8 \times 10^{-4}$ , which is less than the acceptance criteria performance goal of  $2 \times 10^{-4}$ . Thus, this structure meets the probabilistic acceptance criteria specified in DOE Standard 1020.

#### 5. CONCLUSIONS

A methodology to predict structural behavior in older DOE reinforced concrete facilities was implemented. This methodology can be used to demonstrate seismic capability consistent with the performance goals stated in DOE Standard 1020 when traditional deterministic methods indicate deficient seismic designs. Adaptations of the methodology can be used to meet performance goals developed for other nuclear and non-nuclear buildings.

Key to the development of realistic estimates of the ultimate lateral load resisting capacities for existing structures is the understanding of the behavior of reinforced concrete joints with partially developed bars. These joints do not necessarily demonstrate brittle behavior and the limited rotation capability of partially developed joints can contribute significantly to the overall ductility of the reinforced concrete frame. Notwithstanding the ductility available when estimating the limit state, significant damage in the structure is expected to occur, thus new construction should fully develop bars.

This structure has an elastic frequency on the order of 1 to 1.3 Hz, which increases further as the lateral load increases. This high period structure is displacement controlled thus computed drifts are relatively insensitive to the initial structural stiffness and capacity. The drifts are a function of the low frequency displacements in the ground motions.

#### 6. ACKNOWLEDGMENTS

The information contained in this article was developed during the course of work done under Contract No. DE-AC09-89SR18035 with the U.S. Department of Energy.

The analyses presented in this paper were performed by the engineers in the Structural Mechanics Section and the Site Geotechnical Services Department of the Westinghouse Savannah River Company. The generous

guidance provided by Dr. Robert P. Kennedy, Prof. Charles E. Miller, and Prof. Mehta Sozen are gratefully acknowledged.

## 7. REFERENCES

American Concrete Institute, ACI-318-51, *Building Code Requirements for Reinforced Concrete*, 1951.

American Concrete Institute, ACI-318-95, *Building Code Requirements for Structural Concrete and Commentary*, 1995.

APPLIED TECHNOLOGY COUNCIL, ATC-19, "Structural Response Modification Factors", 1995.

APPLIED TECHNOLOGY COUNCIL, FEMA 273, "NEHRP Guidelines for the Seismic Rehabilitation of Buildings", 1996.

APPLIED TECHNOLOGY COUNCIL, FEMA 274, "NEHRP Commentary on the Guidelines for the Seismic Rehabilitation of Buildings", 1996.

Aycardi, A. E., Mander, J. B., and Reinhorn, A. M., "Seismic Resistance of Reinforced Concrete Frame Structures Designed Only for Gravity Loads: Part II - Experimental Performance of Subassemblages, NCEER-92-0028, National Center for Earthquake Engineering Research, December 1992.

Beres, A., White, R., Gergely, P., "Seismic Performance of Interior and Exterior Beam-to-Column Joints Related to Lightly Reinforced Concrete Frame Buildings: Detailed Experimental Results", NCEER-92-0024, National Center for Earthquake Engineering Research, September 1992

DOE-STD-1020-94, "Natural Phenomena Hazards Design and Evaluation Criteria for

Department of Energy Facilities", April 1994.

Eligehausen, R., Popov, E. P., Bectero, V. V., "Local Bond Stress-Slip Relationships of Deformed Bars Under Generalized Excitations," Report UCB/EERC-83/23, October 1983.

Gulkan, P. and Sozen, M.A., "Inelastic Responses of Reinforced Concrete Structures to Earthquake Motions," *ACI Journal*, Vol. 71, No. 12, December, 1974.

International Conference of Building Officials, *Uniform Building Code*, 1994.

Iwan, W. D., "Estimating Inelastic Response Spectra from Elastic Spectra", *Earthquake Engineering & Structural Dynamics*, Vol. 8, 1980.

Kennedy, R.P., et.al. "Engineering Characterization of Ground Motion - Task I: Effects of Characteristics of Free-Field Motion on Structural Response," NUREG/CR-3805, Vol. 1, U.S. Nuclear Regulatory Commission, 1984.

Mertz, G., Loceff, F., Houston, T., Rawls, G., and Mulliken, J., "Performance Based Seismic Qualification of Reinforced Concrete Nuclear Materials Processing Facilities", 6<sup>th</sup> National Conference on Earthquake Engineering, Seattle, May, 1998.

Takeda, T., Sozen, M. A., and Nielson, N. N., "Reinforced Concrete Response to Simulated Earthquakes", *ASCE Journal of the Structural Division*, Vol. 96, No. ST 12., 1970

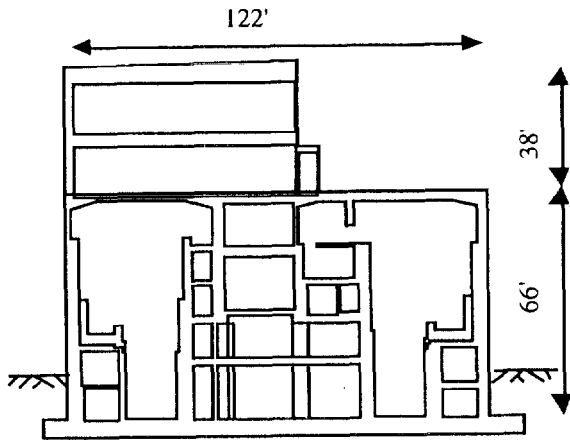


Figure 1. Frame cross section and vertical mass distribution

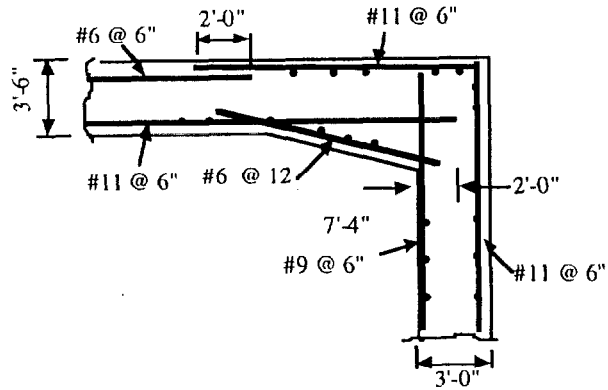


Figure 2. Typical joint detail

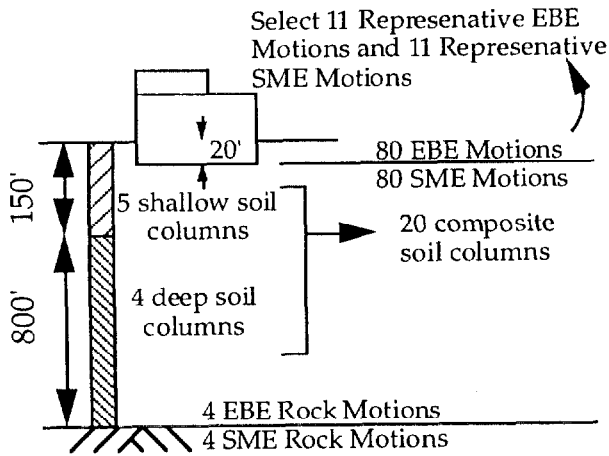


Figure 3. Development of Seismic Input

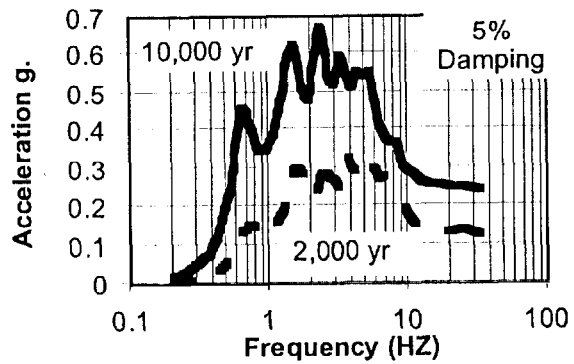


Figure 4. Mean site specific spectra

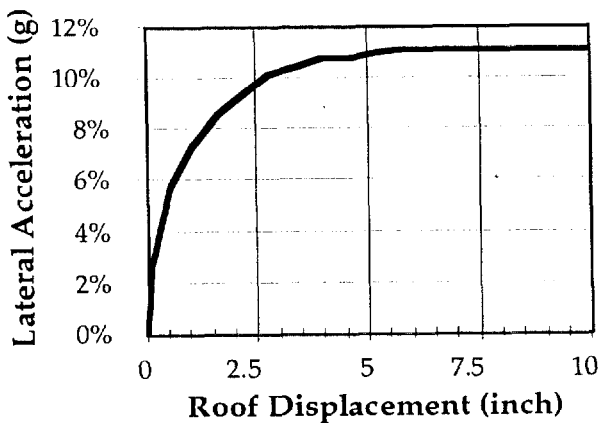


Figure 5. Monotonic load-deformation curve

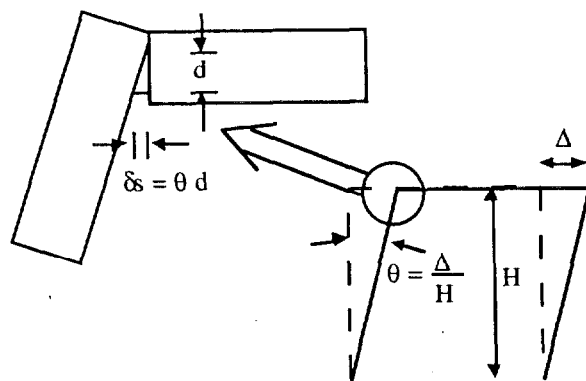


Figure 6. Relationship between bar slip and drift

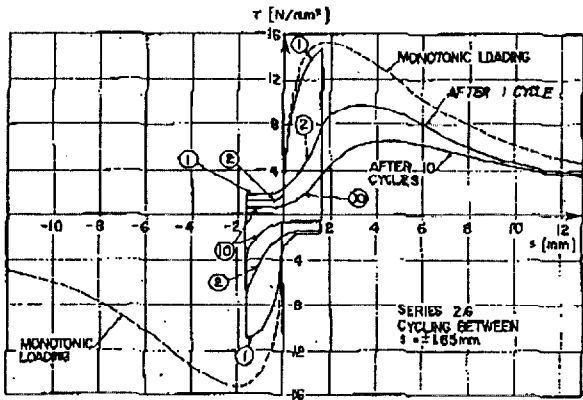


Figure 7. Bar pullout test (Eligehausen, 1983)

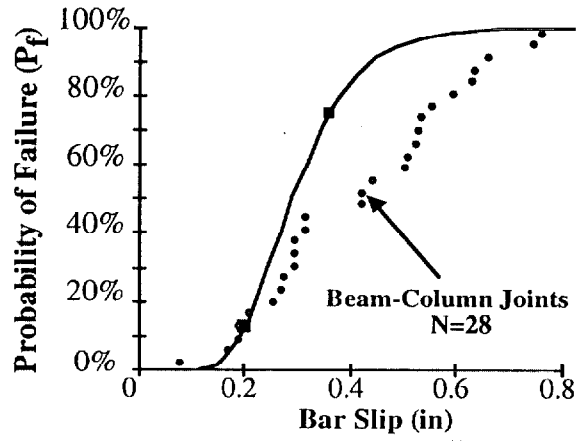


Figure 8. Probability of failure versus bar slip for confined joints

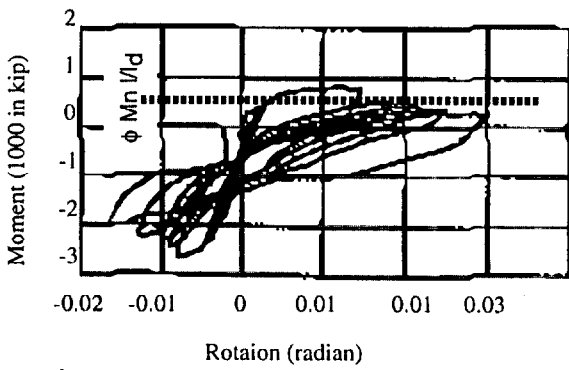


Figure 9. Full scale joint test (Beres, 1992)

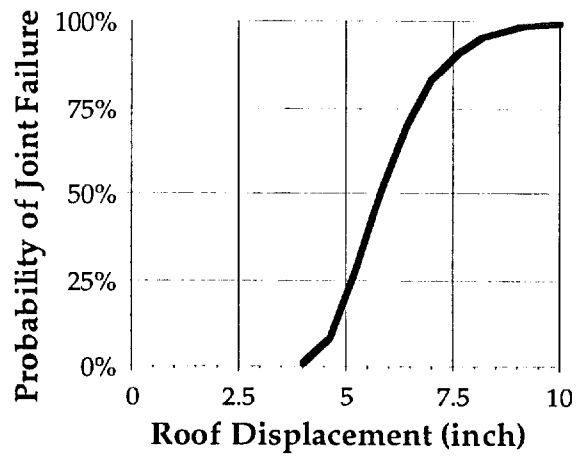


Figure 10. Envelope of joint failure probability versus roof displacement

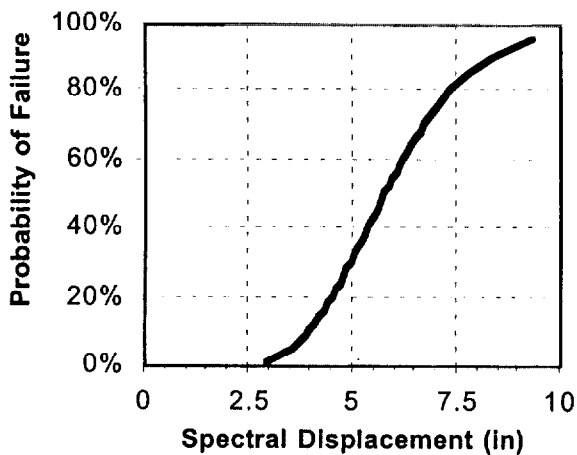


Figure 11. Building fragility curve